THE COMPLEX MODELLING OF VARIOUS EFFECTS OF THE SUB-SLAB VENTILATION SYSTEMS

Z. Svoboda

Czech Technical University, Faculty of Civil Engineering, Department 124, Thákurova 7, 166 29 Praha 6, Czech Republic, e-mail: svobodaz@fsv.cvut.cz

Annotation

The following paper is focused on the possibilities of the numerical modelling of the fields of radon concentration, temperature and relative humidity in the ground under the houses with the sub-slab ventilation systems. The governing equations are briefly discussed as well as their numerical solution using the finite element method. The paper also shows some results of numerical analyses in comparison with the experimental data obtained during measurement of one typical house with the sub-slab ventilation system.

1. Introduction

Sub-slab ventilation systems and mainly sub-slab depressurisation systems (SSD systems) belong among the most effective radon protective and remedial measures. The effectiveness of these systems depends on several key factors – such as floor tightness, vertical profile of soil permeability, fan power and number, location and size of sumps or pipes [1]. Numerical modelling can be very powerful tool in the design stage of such systems – helping for example with the determination of the best layout of ventilation system [2], [3], [4], [5]. Necessary calculations include the estimation of the pressure field in the ground under the house with SSD system and the estimation of the radon concentration field. The SSD system also affects the temperature and relative humidity distribution and therefore also these fields should be additionally calculated. All analyses mentioned above can be carried out with the simplified assumption of the non-transient, steady-state, behavior which is exact enough for the purposes of the SSD systems design. The numerical solution can be obtained by means of the finite difference method or by means of the finite element method, which will be discussed in more detail in this paper.

2. Description of governing equations

2.1. Air pressure field

Three-dimensional steady-state air pressure field in a porous medium can be calculated by means of the well-known partial differential equation

$$k \cdot \nabla^2 P = 0\,, \tag{1}$$

where k is permeability of the porous medium in m^2 and P is pressure in Pa. The boundary condition used for the equation (1) is usually the simple Dirichlet condition. The air flow velocity field is calculated from the Darcy's law

$$\vec{v} = -\frac{k}{\mu_v}\Delta P\,, \tag{2}$$

where μ_v is dynamic viscosity of the air, usually taken as $1{,}7.10^{-5}$ kg/(m.s). Equations (1) and (2) can be used with the assumptions that the air is incompressible and the air flow is laminar. The

second assumption is – according to various sources of information [4], [6], [7] – satisfied if the Reynolds number defined for the case of air flow in a porous material as

$$\mathrm{Re} = \frac{d_c \cdot |\vec{v}|}{\nu} \tag{3}$$

is not higher than the limit value ranging from 1 to 70 (d_c is characteristic diameter of a pore in a porous material in m, $|v|$ is velocity vector magnitude in m/s and ν is kinematical viscosity of the air taken as 1,4 . 10^{-5} m^2/s). It is possible to calculate that the building materials and various types of soil with the permeability lower than 10^{-8} m^2 have Reynolds number under the value of 5 if the loading pressure gradient is within the range from 0 to 50 Pa (assuming that the characteristic diameter of the pores in the material is not higher than 2 mm). This requirement for the maximum pressure gradient is usually met in the case of SSD systems.

Numerical solution of equations (1) and (2) causes no major problems and can be found in several publications, e.g. [8], [9].

2.2. Radon concentration field

The distribution of radon concentration in the soil under the building is governed by one type of the so-called convective-diffusion equation, which can be written for the steady-state case as

$$D_e \nabla^2 C - \frac{1}{\varepsilon} \vec{v} \cdot \Delta C + G - \lambda_r C = 0\,, \tag{4}$$

where D_e is effective radon diffusion coefficient in m^2/s, C is radon concentration in the soil gas in Bq/m^3, ε is porosity of a porous material, $\vec{v}$ is air flow velocity in a porous material in m/s, λ_r is radon decay constant (2,1.10^{-6} 1/s) and G is radon generation rate defined as

$$G = \frac{a_{Ra} \cdot \lambda_r \cdot \rho \cdot f}{\varepsilon}, \tag{5}$$

where a_{Ra} is mass activity of radium Ra^{226} in a material in Bq/kg, ρ is bulk density of a material in kg/m^3 and f is radon emanation coefficient. The radon transport caused by water flow is neglected in the equation (4) due to its minor importance.

The validity of the equation (4) is conditioned by the following assumptions: the convection of air through the building construction is caused only by the pressure difference, the air is incompressible and the air flow is laminar (see also chapter 2.1).

Interesting issue is the definition of the boundary conditions for the equation (4). Most used in practice is the Dirichlet type of boundary condition, which is usually defined on the boundary between the soil and ambient air as

$$C = C_a\,, \tag{6}$$

and in the deep layers of the soil as

$$C = \frac{G}{\lambda_r}. \tag{7}$$

The main problem of easy-to-use Dirichlet boundary condition is in the fact that this condition directly defines the radon concentrations on the boundaries of calculated area. This approach does not lead to substantial errors in radon concentration field in the soil, but on the other hand the error in estimation of the radon exhalation rate from the soil or floor constructions could be considerable high due to the fact that the radon concentration right on the surface of radon-productive soil or floor is always higher than the radon concentration in the ambient air.

Therefore in the cases of evaluation of radon protective measures, Newton type of boundary condition should be used – preferably in the following form

$$-\varepsilon \cdot D_e \frac{\partial C}{\partial n} + v_n \cdot C = h_r \cdot (C - C_a), \tag{8}$$

where $\partial/\partial n$ is derivative in the direction of the external normal to the boundary, v_n is velocity component normal to the boundary in m/s, C_a is radon concentration in the ambient air in Bq/m^3 and h_r is radon transfer coefficient, which can be defined as

$$h_r = \frac{D_o}{b}, \tag{9}$$

where D_o is radon diffusion coefficient in the air (1,1.10^{-5} m^2/s). The thickness of the transfer layer b defines the distance in which the radon concentration on the soil surface C decreases to the level of the radon concentration in the ambient air C_a. This value can be calculated according to J. Nemec [10] as

$$b = \sqrt{\frac{D_o}{\lambda_r}} \cdot \frac{\varepsilon \cdot D_e}{D_o}, \tag{10}$$

with the values of ε and D_e characterising the top-most layer of the soil or of the floor.

The solution of the equation (4) can be found by means of the finite element method using the Petrov-Galerkin process. This approach, which is also known as the streamline balancing diffusion or streamline Petrov-Galerkin process, is based on a special selection of the vector of weighting functions W different from the vector of interpolation functions N. More details of this derivation process and discussion on the numerical stability can be found in [2]. The finite element formulation of the discussed problem can be written in the form

$$(K_D + K_{vr} + K_{\lambda r} + K_{hr}) \cdot C = q_{hr} + q_G, \tag{11}$$

where the radon conductance matrix K_D is defined as

$$K_D = \int_{\Omega^{(e)}} D_e \cdot \Delta W \cdot \Delta N^T \, \mathrm{d}\Omega, \tag{12}$$

the radon convective transport matrix K_{vr} as

$$K_{vr} = \int_{\Omega^{(e)}} \frac{1}{\varepsilon} (\vec{v} \cdot W \cdot \Delta N^T) \mathrm{d}\Omega, \tag{13}$$

the radon radioactive decay matrix $K_{\lambda r}$ as

$$K_{\lambda r} = \int_{\Omega^{(e)}} \lambda_r \cdot W \cdot N^T \mathrm{d}\Omega, \tag{14}$$

the radon boundary conditions matrix K_{hr} as

$$K_{hr} = \int_{\Gamma^{(e)}} \left(h_r - \frac{v_n}{\varepsilon} \right) \cdot W \cdot N^T \, \mathrm{d}\Gamma, \tag{15}$$

the radon boundary conditions vector q_{hr} as

$$q_{hr} = \int_{\Gamma^{(e)}} \left(h_r - \frac{v_n}{\varepsilon} \right) \cdot W \cdot \overline{C} \, \mathrm{d}\Gamma \tag{16}$$

and the radon generation rate vector q_G as

$$q_G = \int_{\Omega^{(e)}} G \cdot W \mathrm{d}\Omega . \tag{17}$$

Note that the radon convective transport matrix K_{vr} is asymmetrical and so the final linear equations system for unknown nodal values C always has asymmetrical matrix.

2.3. Temperature field

The heat transfer in the soil under the building with SSD system cannot be taken as the simple heat conduction. The heat transfer caused by convection is also very important in this case and thus the combined heat transfer must be taken into account. The partial differential equation governing this process can be for steady-state case stated as

$$\lambda \cdot \nabla^2 \theta - \rho_a c_a \cdot \vec{v} \cdot \Delta\theta = 0 , \tag{18}$$

where λ is thermal conductivity in W/(m.K), θ is temperature in K, ρ_a is density of the air (1,2 kg/m^3) and c_a is thermal capacity of the air (1010 J/(kg.K)).

The first term on the left-hand side of the equation (18) represents the heat transport due to conduction; the second term represents the heat transport due to convection. The most used boundary condition for the equation (18) is Newton boundary condition defined as

$$-\lambda \frac{\partial \theta}{\partial n} + v_n \rho_a c_a \left(\theta - \overline{\theta}\right) = h \cdot \left(\theta - \overline{\theta}\right), \tag{19}$$

where h is heat transfer coefficient in W/(m^2.K) and $\overline{\theta}$ is known ambient temperature at the boundary in K.

The numerical solution of the equation (18) has been derived by means of the finite element method (again using the Petrov-Galerkin process) with assumptions that the convection of air through the building construction is caused only by the pressure difference, the air is incompressible and the air flow is laminar (for more details see chapter 2.1). Detailed discussion of this derivation including numerical stability analysis can be found in several previously published works [11], [12]. The general finite element formulation is

$$\left(K_\lambda + K_v + K_h\right) \cdot \theta = q_h . \tag{20}$$

The conductance matrix K_λ is defined as

$$K_\lambda = \int_{\Omega^{(e)}} \lambda \cdot \Delta W \cdot \Delta N^T \, \mathrm{d}\Omega , \tag{21}$$

the convective transport matrix K_v as

$$K_v = \int_{\Omega^{(e)}} \rho_a c_a \cdot \vec{v} \cdot \Delta N^T \, \mathrm{d}\Omega , \tag{22}$$

the boundary conditions matrix K_h as

$$K_h = \int_{\Gamma^{(e)}} \left(h - v_n \rho_a c_a\right) \cdot W \cdot N^T \, \mathrm{d}\Gamma \tag{23}$$

and the boundary conditions vector q_h as

$$q_h = \int_{\Gamma^{(e)}} \left(h - v_n \rho_a c_a\right) \cdot W \cdot \overline{\theta} \, \mathrm{d}\Gamma . \tag{24}$$

The vector of the weighting functions W must be again different from the vector of interpolation functions N and could be derived using the process recommended in [8].

Note again that the convective transport matrix K_v is asymmetrical, which leads to the asymmetrical matrix of the linear equations system.

2.4. Relative humidity field

The humidity distribution in the ground under the building with SSD system is governed by another type of convective-diffusion equation:

$$\frac{D}{\mu}\cdot\nabla^2\rho_h - \vec{v}\cdot\Delta\rho_h = 0\,, \tag{25}$$

where μ is vapor resistance factor of the material, ρ_v is partial water vapor density in kg/m^3 and D is water vapor diffusion coefficient in air in m^2/s, which can be calculated for example from:

$$D = 2{,}17\cdot10^{-5}\left(\frac{T}{273{,}15}\right)^{1{,}88}, \tag{26}$$

where T is absolute temperature of the air in K.

The most used boundary condition for the equation (25) is again Newton boundary condition – this time defined as

$$-\frac{D}{\mu}\frac{\partial\rho_h}{\partial n} + v_n\cdot\rho_h = \beta\cdot\left(\rho_h - \overline{\rho}_h\right), \tag{27}$$

where $\overline{\rho}_h$ is known ambient partial water vapor density at the boundary in kg/m^3 and β is water vapor transfer coefficient in m/s, which is defined as

$$\beta = 2{,}04\cdot10^{-6}\cdot h\cdot r\,, \tag{28}$$

where h is heat transfer coefficient in W/(m^2.K) and r is gas constant pro water vapor (461,9 J/(kg.K)).

Partial water vapor density $\overline{\rho}_h$ can be determined from the known temperature and relative humidity using the equations

$$\rho_h = \frac{\varphi\cdot\rho_{sat}}{100} \text{ and } \rho_{sat} = \frac{p_{sat}}{461{,}9\cdot\left(273{,}15+\theta\right)}, \tag{29}$$

where φ is relative humidity in %, p_{sat} is saturated partial water vapor pressure in Pa and θ is temperature in °C.

The numerical solution of equation (25) has been derived again using the finite element method with the same assumptions as in previous cases. The general finite element formulation is

$$\left(K_D + K_V + K_\beta\right)\cdot\rho_h = q_\beta\,. \tag{30}$$

The diffusion matrix K_D is defined as

$$K_D = \int_{\Omega^{(e)}}\frac{D}{\mu}\cdot\Delta W\cdot\Delta N^T\,\mathrm{d}\Omega\,, \tag{31}$$

the convective transport matrix K_v as

$$K_v = \int_{\Omega^{(e)}}\vec{v}\cdot\Delta N^T\,\mathrm{d}\Omega\,, \tag{32}$$

the boundary conditions matrix K_β as

$$K_\beta = \int_{\Gamma^{(e)}} (\beta - v_n) \cdot W \cdot N^T \, \mathrm{d}\Gamma \tag{33}$$

and the boundary conditions vector q_β as

$$q_\beta = \int_{\Gamma^{(e)}} (\beta - v_n) \cdot W \cdot \overline{\rho}_h \, \mathrm{d}\Gamma \,. \tag{34}$$

The result of the numerical solution of equation (30) is the field of partial water vapor densities. The relative humidity field can be afterwards easily calculated using equations (29) and the results of the temperature field calculation.

3. Verification of models

The reliability of the presented numerical models has been verified on six houses with different types of SSD systems. Data for the comparison between the calculation and the experiment has been taken from [13]. The results obtained from one measured house are further presented to demonstrate the whole process of verification.

3.1 Experimental house

The chosen single-family house was located at Milesov, Czech Republic. The house was around 100 years old and had three habitable rooms in the ground floor (Fig. 1). The mean indoor radon concentration in the house was 1550 Bq/m^3. The remediation of the house was based on the installation of the SSD system in combination with the reconstruction of floors (old concrete floor slabs were replaced by the new ones, 50 mm thick thermal insulation was added). Perforated pipes were laid directly to the drainage layer of highly permeable gravel. The layout and diameters of pipes can be seen on Fig. 1. Perforated pipes were connected to the vertical exhaust pipe that was inserted into a free flue and ended with a roof fan above the chimney.

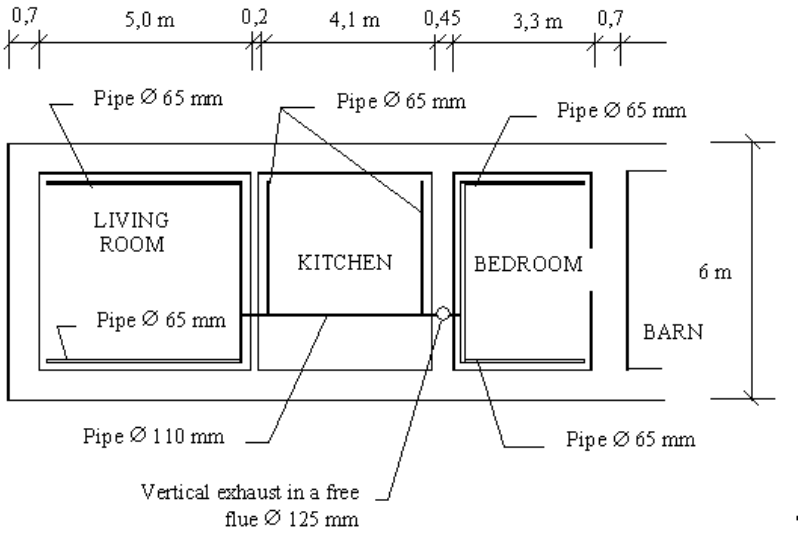

Fig. 1 The layout of the perforated pipes in the experimental house

During the measurements the house was in ordinary use by the owner's family. Soil air temperature, relative humidity, pressure difference and soil air radon concentration were measured continuously. All measurements were carried out for both possible cases: during the period when the SSD system was switched off and for the case with SSD system in operation. Simultaneously, the indoor air temperature, indoor radon concentration and outdoor air

temperature were also registered. Important part of the experiment was also a detailed investigation of the building site in order to obtain necessary data for the verification of simulation models. Material characteristics used in the numerical simulations are summarized in Tab. 1.

Tab. 1 Material characteristics

Measured material	Permeability	Porosity	Radon diffusion coefficient	Radon generation rate	Thermal conductivity
Drainage layer	1.10^{-9} m^2	0.30	9.10^{-6} m^2/s	---	1.8 W/(m.K)
Concrete floor construction	1.10^{-16} m^2	0.10	1.10^{-8} m^2/s	---	1.5 W/(m.K)
Concrete foundations	1.10^{-16} m^2	0.10	1.10^{-8} m^2/s	---	2.1 W/(m.K)
Thermal insulation	1.10^{-14} m^2	0.30	1.10^{-7} m^2/s	---	0.04 W/(m.K)
Soil layer in the depth from 0 to 1 m	15.10^{-13} m^2	0.30	1.10^{-6} m^2/s	5.10^{-5} kBq/(m^3.s)	1.9 W/(m.K)
Soil layer in the depth from 1 to 3 m	1.10^{-11} m^2	0.30	2.10^{-6} m^2/s	12.10^{-5} kBq/(m^3.s)	2.0 W/(m.K)

3.2 Numerical model geometry and boundary conditions

The geometry of the numerical model of the floor and the soil beneath it was derived from the plan of the house and from the layout of pipes (see Fig. 1). The circular pipes were replaced in the model by the pipes with a square cross-section. Pressure loss due to friction in the pipes was incorporated to the calculation in a simplified way by means of their permeability ($k=3.10^{-8}$ m^2). The soil under the house was modelled as a large block reaching in the horizontal direction 1 m beyond the perimeter walls. In the vertical direction, the depth of this block was taken as 2 m (for the pressure difference calculation) or 3 m (for the temperature, relative humidity and radon concentration calculations). In accordance with the site investigation, two soil layers of different permeability were considered. The dimensions of the floor slab and foundations were taken according to the real house.

The boundary conditions used in the calculations were defined as close to measured data as it was possible. Their overview can be found in Tab. 2. At the bottom of the vertical exhaust pipe, the under-pressure of –65 Pa was considered again according to measured value.

Tab. 2 Boundary conditions

Parameter	Position of the boundary condition		
	Soil surface	Floor surface	Deep soil
Relative pressure [Pa]	0	-2	-6
Radon concentration [kBq/m^3]	0.01	0.10	57
Radon transfer coefficient [m/s]	18.10^{-5}	53.10^{-3}	10 000
Temperature [°C]	5	22	5
Heat transfer coefficient [W/(m^2.K)]	23	6	10 000

3.3 Results of numerical modeling in comparison with the measured data

The three-dimensional air pressure field in the whole sub-slab space of the experimental house at Milesov was calculated by means of the computer program Tlak3D. The calculation procedure of this software tool is described in chapter 2.1; properties of materials and boundary conditions used in calculation can be found in Tab. 1 and Tab. 2.

One example of the results of air pressure field calculation for the case of fan operation with under-pressure of –65 Pa in the exhaust pipe is shown in Fig. 2. The measuring points are also marked in the same figures. Each black dot represents one measuring point together with the measured value of under-pressure for the considered boundary conditions. It can be seen that the correlation between calculated and measured values is very good – differences are not higher than 10 %.

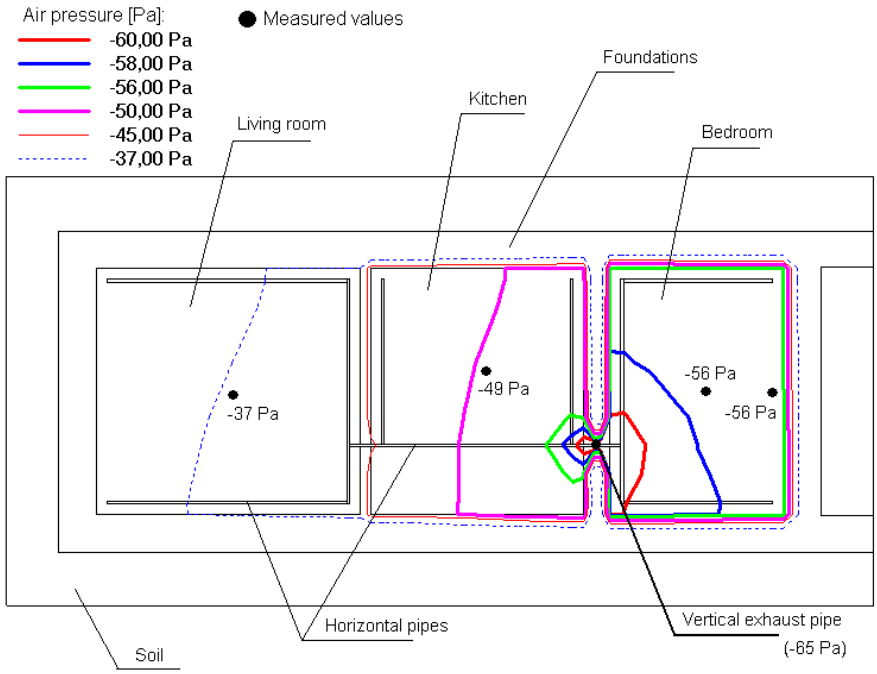

Fig. 2 Two-dimensional view of calculated pressure field in the drainage layer

The two-dimensional steady-state temperature and relative humidity fields in the soil under the experimental house were calculated by means of the program Wind2D. The theoretical background of this software is discussed in chapter 2.3 and 2.4. Boundary conditions and the properties of the soil and building materials are summarised in Tab. 1 and Tab. 2.

The calculation of the temperature and relative humidity fields was carried out twice – once for the case with the SSD system in operation and once for the case with the fan switched off. The results of calculation for the ventilated soil can be seen in Fig. 3, which represents the cross section through the sub-slab region under the living room. For the working cycle the temperature distribution was determined using the mean under-pressure of –37 Pa as the boundary condition in the perforated pipes located in the drainage layer. This value was derived from the results of three-dimensional pressure field calculation (see Fig. 2) and it is also in a good agreement with the measured value. All other boundary conditions were taken according to Tab. 2.

The points with temperatures measured in-situ are marked again with the black dots in Fig. 3. As can be seen from the figure, the differences between measured and calculated values are up to 15 %. Model predictions as well as the measured data show very clearly the effect of soil ventilation on the sub-floor temperatures. If the soil is ventilated by continuously operating fans, the decrease of temperatures under the floor slab with 50 mm thick thermal insulation can be as high as 2 °C. The theoretical model shows also – in the same way as the measured data do – the negative effect of thermal bridges on the perimeter of the house (un-insulated foundations). The temperatures in the drainage layer in the vicinity of perimeter walls are approximately 1 °C lower than those in the same layer in the middle of the house.

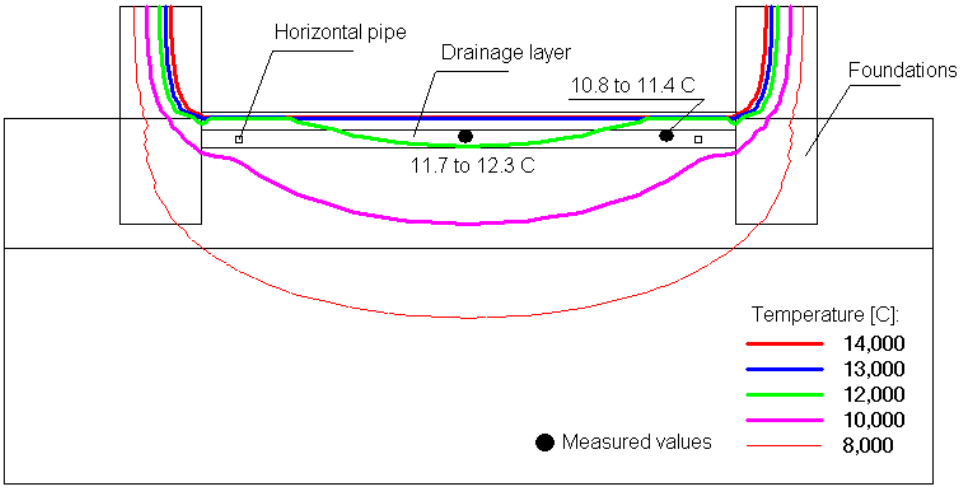

Fig. 3 Calculated temperature distribution in the sub-slab region – case of SSD system in use

The relative humidity field calculation shows increase of the relative humidity values in the drainage layer in case of SSD system in use. When the SSD system is switched off, the relative humidity in the drainage layer varies between 68 and 73%. With the SSD system in use, the relative humidity climbs up to even 83% in the areas close to horizontal pipes. These results, which are presented in Fig. 4, are generally in good correspondence with the measured data, although the experimentally obtained results show a little lower values of relative humidity (approximately 30-70% in the center of the room and 70-90% near the walls).

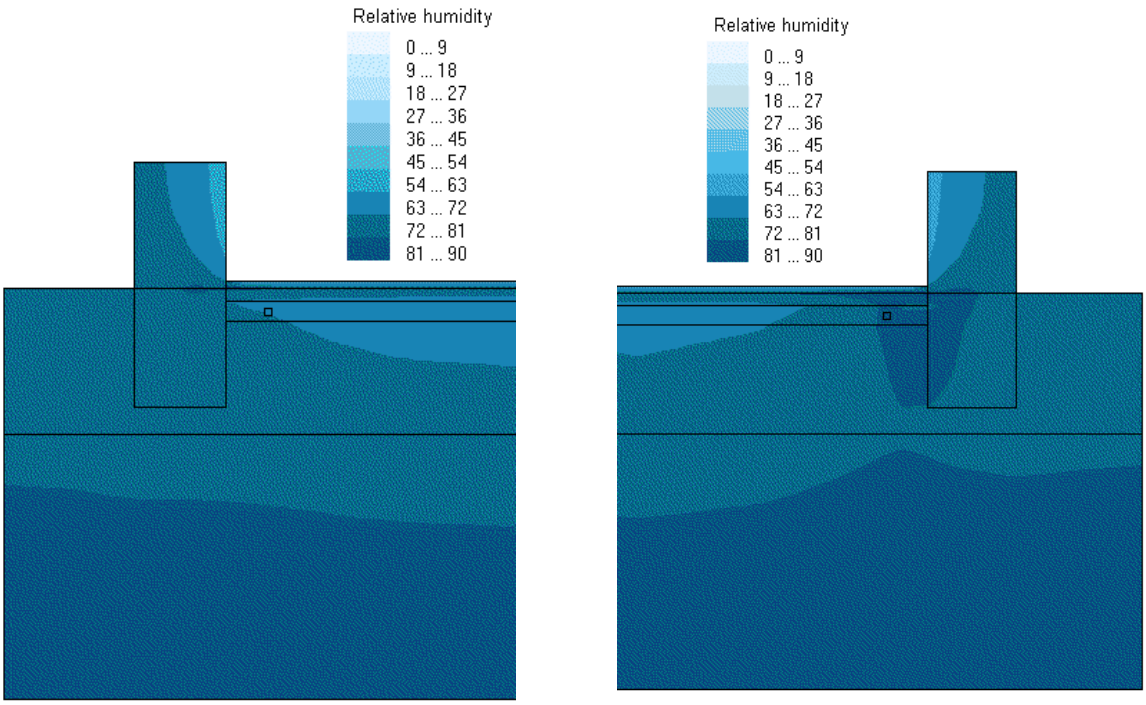

SSD system out of operation SSD system in operation

Fig. 4 Calculated relative humidity distribution in the sub-slab region

Finally, the two-dimensional steady-state field of radon concentrations in the soil under the experimental house was calculated by means of the finite element model described in chapter

2.2. The properties of materials and boundary conditions considered in the calculation are presented in Tab. 1 and Tab. 2. The under-pressure in the perforated pipes was introduced in the calculation exactly in the same way as in the case of temperature field calculation.

Some results of radon concentration field calculation obtained by means of the software Radon2D are presented in Fig. 5. The correlation between measured and calculated values of radon concentration is worse than in the cases of temperature and air pressure fields – differences range from 20 to 85 %. Nevertheless, the trends in radon concentration distribution are simulated in the numerical model with a sufficient reliability. The calculation for example shows that the radon concentration in the drainage layer decreases as a result of the soil ventilation from the mean value of 23 kBq/m^3 (SSD system switched off) to the mean value of 14 kBq/m^3 (SSD system in use). This result corresponds with the general trends obtained from the measurement.

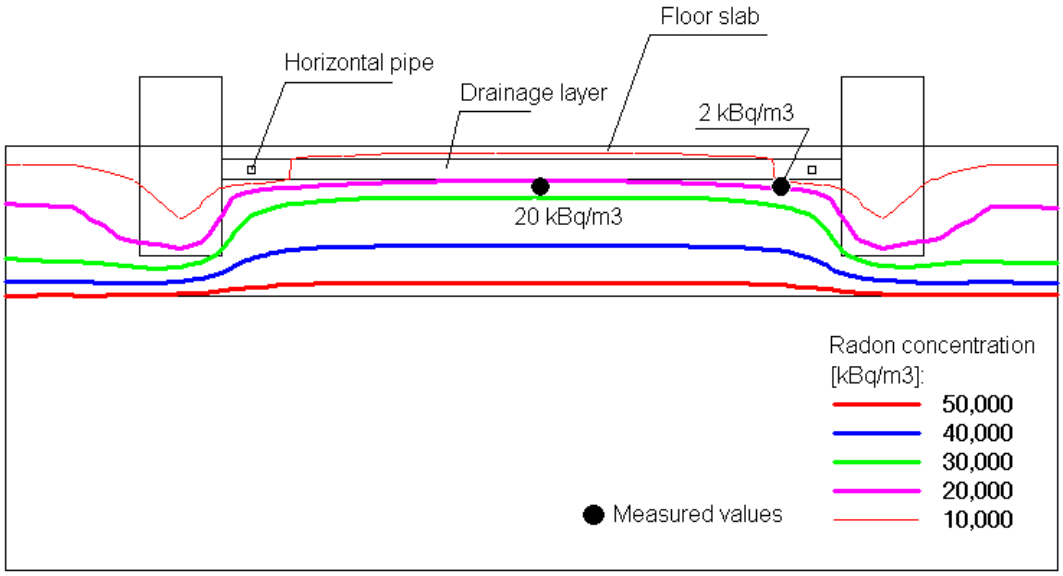

Fig. 5 Calculated radon concentration field in the sub-slab region – case of SSD system in use

3.4 Brief summary of results

The completed verification of numerical models shows that the highest reliability can be expected from the model for three-dimensional pressure field calculations (program Tlak3D). The maximum difference between the calculated and measured air pressure values was for this model only 10%.

On the other hand, the lowest accuracy was found out for the numerical model for the assessment of radon concentrations. Here the maximum difference between measured and calculated values reached the level of 85 %. The fact that this calculation procedure is not so precise can be caused by several factors, such as: simplification of the calculation to the two-dimensional model, lower accuracy of numerical solution of the governing equation, insufficient accuracy of used soil properties. The numerical model of Radon2D software can be therefore recommended preferably for the calculations of the trends of radon concentration distribution rather than for accurate calculations. Nevertheless, this conclusion does not decrease the applicability of numerical modelling in the field of soil ventilation, because it is much better to derive the design of SSD systems from predicted under-pressures than from expected decrease of radon concentrations.

This paper has been partly supported by the Research Project No. 211100001 Functional qualification and optimization of building structures.

References

[1] Jiranek M.: Efficiency and Side Effects of Sub-slab Depressurisation Systems. In: Radon Investigations in the Czech Republic IX, 2002, pp. 87-94.

[2] Jiranek M., Svoboda Z.: Verification of Radon Protective Measures by Means of a Computer Model. In: Proceedings of the 5th Int. IBPSA Building Simulation Conference, Vol. II, Prague 1997, pp. 165-172.

[3] Jiranek M., Svoboda Z.: The Computer Model for Simulation of Soil Ventilation Systems Performance. In: Proceedings from the European Conference on Protection against Radon at Home and at Work, Prague 1997, pp.110-113.

[4] Bonnefous, Y.C., Gadgil, A.J., Fisk, W.J, Prill, J.R., Nematollahl, A.R.: Field Study and Numerical Simulation of Sub-slab Ventilation Systems, In: Environmental Science and Technology, Vol. 26, 1992, pp. 1752-1759.

[5] Andersen, C.E., Albarracin, D., Csige, I., Graaf, E.R., Jiranek, M., Rehs, B., Svoboda, Z., Toro L.: ERRICCA Radon Model Intercomparison Exercise, Riso National Laboratory, Roskilde 1999.

[6] Gadgil, A.J., Bonnefous, Y.C., Fisk, W.J.: Relative Effectiveness of Sub-slab Pressurisation and Depressurisation Systems for Indoor Radon Mitigation – Studies with an Experimentally Verified Numerical Model. In: Indoor Air, Vol. 4, 1994, pp. 265-275.

[7] Nazaroff, W.W., Sextro, R.G.: Technique for Measuring the Indoor ^{222}Rn Source Potential in Soil, In: Environmental Science and Technology, Vol. 23, 1989, pp. 451-458.

[8] Zienkiewicz, O.C., Taylor, R.L.: The Finite Element Method, Fourth Edition, Vol. 1 & 2, McGraw - Hill Book Company, London 1991.

[9] Huebner, K.H., Thornton, E.A.: The Finite Element Method for Engineers, John Wiley & Sons, New York 1982.

[10] Jiranek, M.: Building Constructions – Radon Protective Measures, Czech Technical University, Prague 2000 (in Czech).

[11] Svoboda, Z.: The Convective-Diffusion Equation and its Use in Building Physics, In: International Journal on Architectural Science. Vol. 1, No. 2 (2000), pp. 68-79.

[12] Svoboda, Z.: The Analysis of the Convective-Conductive Heat Transfer in the Building Constructions, In: Proceedings of the 6th Int. IBPSA Building Simulation Conference, Vol. I, Kyoto 1999, pp. 329-335.

[13] Jiranek, M., Schreyer, J.: Applicability of Sub-Slab Depressurisation Systems Beneath Existing Houses. Final Research Report for the State Office for Nuclear Safety and the Ministry of Industry and Commerce, Prague 2002 (in Czech).